Mon. Not. R. Astron. Soc. **000**, 000–000 (2001) Printed 1 February 2008 (MN LATEX style file v2.2)

The massive double-lined O-type binary HD 165052

J.I. Arias[1⋆], N.I. Morrell[1]†, R.H. Barbá[1†], G.L. Bosch[1]‡, M. Grosso[2]§, M. Corcoran[3]
[1] *Facultad de Ciencias Astronómicas y Geofísicas, Universidad Nacional de La Plata, Paseo del Bosque S/N, B1900FWA La Plata, Argentina*
[2] *Complejo Astronómico El Leoncito, Av. España 1512 sur, 5400 San Juan, Argentina*
[3] *Universities Space Research Association, 7501 Forbes Blvd, Ste 206, Seabrook, MD 20706, USA &*
Laboratory for High Energy Astrophysics, Goddard Space Flight Center, Greenbelt MD 20771, USA

1 February 2008

ABSTRACT
We present a new optical spectroscopic study of the O-type binary HD 165052 based on high- and intermediate-resolution CCD observations. We re-investigated the spectral classification of the binary components, obtaining spectral types of O6.5 V and O7.5 V for the primary and secondary, respectively, finding that both stars display weak C III λ5696 emission in their spectra. We also determined a radial-velocity orbit for HD 165052 with a period of 2.95510 ± 0.00001 d, and semiamplitudes of 94.8 and 104.7 ± 0.5 km s^{-1}, resulting in a mass ratio $Q = 0.9$. From a comparison with previous radial-velocity determinations, we found evidence of apsidal motion in the system. Several signatures of wind-wind collision, such as phase-locked variability of the X-ray flux and the Struve-Sahade effect, are also considered. It was also found that the reddening in the region should be normal, in contrast with previous determinations.

Key words: stars: binaries – stars: early-type – stars: individual: HD 165052 – X-rays: stars

1 INTRODUCTION

NGC 6530 is a very young open cluster located in the central part of the H II region M 8 (the Lagoon Nebula, which contains also the NGC 6523 nebula). NGC 6530 is one of the more studied clusters in our Galaxy. It has an interesting history of star formation which apparently is still in progress (Sung, Chun & Bessel 2000).

One of the O-type members of NGC 6530 is the double-lined binary HD 165052 (= HIP 88581 = CD-24 13864; $\alpha_{2000} = 18^{\rm h}05^{\rm m}11^{\rm s}$, $\delta_{2000} = -24^\circ23'54''$; $V = 6.87$). This star is refered as #118 in the pioneering work of Walker (1957) on this young open cluster. The first indication of variable radial velocity in HD 165052 was given by Plaskett (1924), while its double-lined binary nature was pointed out by Conti (1974). The first orbital solution for this binary system was obtained by Morrison & Conti (1978), based on 20 photographic spectrograms at a reciprocal dispersion of 17 Å mm^{-1}. HD 165052 was classified as O7: by Conti (1974) and O6.5 V + O6.5 V by Morrison & Conti (1978). Because of the relatively modest resolution of their observations in addition to the remarkable similarities between the two binary components, in terms of both spectral type and linewidths, they were unable to unambiguously distinguish the two components in any individual observation. This led them to derive a period of 6.14 d for the system, essentially doubling the true value. Later, Stickland, Lloyd & Koch (1997), showed that the real period was close to three days, based on 15 high-resolution *IUE* spectra, some of them obtained during four consecutive days.

Regarding the spectral classification of HD 165052, Walborn (1972) derived a spectral type O6.5 V, later modified to O6.5 V(n)((f)) by the same author (Walborn 1973). The designation ((f)) indicates the presence of very weak N III λ4634-40-42 Å emission. As a result of their significant resemblance, the same spectral type has been often adopted for both binary components, i.e. the system has been classified as O6.5 V + O6.5 V, and more recently, O6 V + O6 V (Penny 1996).

Further interest in this system arises from the fact that it is observed as an X-ray source. X-ray emission in early-type binary systems appears as a natural consequence of stellar wind-wind interactions (Chlebowski & Garmany 1991). In such a case, the observed emission is expected to present orbital-phase-related variations. The analysis of such phenomena obviously requires good knowledge of the orbital parameters, and it is important since it provides valuable information about the mass-loss rates and the terminal ve-

⋆ Fellow of the Universidad Nacional de La Plata, Argentina
† Member of Carrera del Investigador Científico, CONICET, Argentina
‡ Post-doctoral fellow of CONICET, Argentina
§ Member of the Carrera del Técnico of CONICET, Argentina

Table 1. Instrumental configurations for different observing runs.

Id.	Date	Spectrograph	Spectral Range [Å]	S/N	No. Obs.
1	1994 June	B&C	3900-4700	100	17
2	1995 May	REOSC-CD	3750–7600	140	5
3	1995 Aug	REOSC-CD	3750–7600	140	7
4	1996 June	REOSC-CD	3750–7600	140	6
5	1996 July	REOSC-SD	3950–7000	320	2
6	1996 Aug	REOSC-CD	3750–7600	140	4
7	1996 Sep	REOSC-CD	3750–7600	140	2
8	1997 Aug	REOSC-CD	3750–7600	140	2
9	2000 June	REOSC-CD	3750–7600	140	12
		REOSC-SD	3950–7000	320	4
10	2001 June	REOSC-CD	3300–6000	140	12

locities of the stellar winds. Corcoran (1996) analyzed the X-ray emission from hot, massive stars. HD 165052 was one of the selected targets in which he detected the presence of phase-dependent variations probably associated with wind-wind collision.

Another expected consequence of colliding winds is the detection of emission in the Hα line. A search for Hα emission in early-type binary systems recently performed by Thaller (1997) yielded negative results for HD 165052.

In this paper we present a new spectroscopic investigation of HD 165052 based on high- and intermediate-resolution CCD observations. From high-resolution optical echelle CCD spectra we have determined the radial-velocity orbit of HD 165052. We have also used those echelle CCD observations and additional intermediate-resolution, high signal-to-noise Cassegrain CCD spectra to review the spectral classification of the binary components of HD 165052. Spectral-type variations related to the Struve-Sahade effect are also described.

2 OBSERVATIONS

All the observations used in the present study were obtained at the Complejo Astronómico El Leoncito (CASLEO [1]), Argentina, with the 2.15-m Jorge Sahade Telescope between June 1994 and June 2001.

The whole data-set contains 73 CCD spectra of HD 165052 with different dispersions and spectral ranges (see Table 1).

The Boller & Chivens (B&C) spectrograph was used with a Thomson 400 × 592 CCD as detector, and a 1200 l mm^{-1} diffraction grating in its second order, yielding a reciprocal dispersion of 0.6 Å px^{-1} and a resolution $R = \lambda/\Delta(\lambda)$ of 3500. The approximate wavelength ranges covered with this configuration were 3900 to 4200 Å and 4400 to 4700 Å, in two different grating angles. A He-Ar lamp was used as comparison source.

For the échelle spectra obtained with the modified REOSC SEL [2] Cassegrain spectrograph in crossed-dispersion mode (REOSC-CD), a Tek 1024 pixel CCD was used as detector. The reciprocal dispersion of these data is 0.17 Å px^{-1} at 4500 Å and they have $R \sim 15000$. 45 of them cover the approximate wavelength region 3800 to 6400 Å, whereas five cover the region from 5200 to 7600 Å. The comparison spectra were obtained with a Th-Ar lamp.

For the spectra secured with the REOSC SEL spectrograph in simple dispersion mode (REOSC-SD), the same detector was used with a 600 l mm^{-1} diffraction grating, this combination yielding a reciprocal dispersion of 2.5 Å px^{-1} and a resolution $R \sim 1800$, and covering wavelength regions from 3900 to 5500 Å and from 5400 to 7000 Å for two different grating positions. A Cu-Ar lamp was used as comparison source for this instrumental configuration.

The usual sets of bias, flat-fields and darks were also secured for each observing night. The data were reduced and analyzed at La Plata Observatory with IRAF[3] standard routines.

3 ORBITAL ELEMENTS AND THEIR DISCUSSION

3.1 Radial Velocities

In order to determine an accurate radial-velocity orbit for the HD 165052 binary system, we used only the high-resolution échelle CCD observations. The high signal-to-noise ratio (S/N) of our échelle data allowed the detection of slight spectral differences between the binary components that will be discussed in section 4.

The radial velocities were measured by interactive fitting of Gaussian profiles to the observed absorption lines. Depending on the degree of blending, we applied simple or simultaneous Gaussian fitting to the absorption-line profiles. For the radial-velocity orbit calculation we considered only those spectra in which the lines of both binary components were resolved.

He I absorption lines, in particular $\lambda\lambda$ 3819, 4026, 4471, 4921, 5015 and 5875, showed well defined profiles and they were measured in almost all cases. Being intrinsically wider, He II $\lambda\lambda$ 4200, 4542, 4686 and 5411 absorption lines were taken into account only when the separation between binary components was maximum. Other lines measured for radial velocities were Si IV λ 4088, O III λ 5592 and C IV $\lambda\lambda$ 5801, 5812. Table 2 shows the complete set of lines measured in each spectrum. For each Julian date, the first and the second lines list the heliocentric radial velocities assigned from the different spectral lines to the primary and secondary components, respectively. There is only one set of measurements for single-lined spectra, which are presumably blended and consequently were omitted from the orbital solution. All the radial velocities are expressed in km s^{-1}. The values labeled as V_R (column 19) were computed as the simple average of the heliocentric radial velocities for the selected lines. The corresponding standard deviations for these averages are shown in column 20. Table 3 shows the final observed radial velocities for the spectra considered in the orbital solution. The column labeled as n shows the number of lines averaged in each case. The orbital phases listed in Table 3 were computed with the ephemeris presented in Table 4.

[1] CASLEO is operated under agreement between CONICET and the National Universities of La Plata, Córdoba and San Juan

[2] Spectrograph Echelle Liège (jointly built by REOSC and Liège Observatory and on long term loan from the latter).

[3] IRAF is distributed by NOAO, operated by AURA, Inc., under agreement with NSF.

Table 2: High-resolution radial velocity measurements for HD 165052.

HJD 2 400 000+	He I 3819	He I 4026	Si IV 4088	He II 4200	He I 4387	He I 4471	Mg II 4481	He II 4542	He II 4686	He I 4713	He I 4921	He I 5015	He II 5411	O III 5592	C IV 5801	C IV 5812	He I 5875	V_R km s^{-1}	σ km s^{-1}
∗49852.677	–	–	–	–	–	−21.7	–	−8.0	–	−9.9	–	+3.1	+5.4	−0.9	–	–	–	−5.3	10.0
∗49853.672	–	–	–	–	–	+5.6	–	–	+10.4	+7.2	–	+17.3	+8.3	–	–	–	–	+9.8	4.5
49854.640	–	+78.0	–	–	–	+94.9	–	–	–	+90.6	–	–	+89.5	–	–	–	–	+88.2	7.2
	–	−95.5	–	–	–	−99.6	–	–	–	−98.4	–	–	−100.7	–	–	–	–	−98.5	2.2
∗49855.651	–	–	+11.9	–	–	+5.5	–	+4.8	−7.7	–	+13.9	–	–	–	–	–	–	+5.7	8.5
49931.634	–	+61.2	+75.2	–	–	+66.3	–	–	–	–	–	+71.0	–	+69.0	+59.1	+71.9	+80.1	+69.2	6.9
	–	−87.0	−90.6	–	–	−89.4	–	–	–	–	–	−107.9	–	−82.8	−96.5	−99.0	−78.2	−91.4	9.5
49932.663	−80.7	−76.3	−73.4	–	–	−75.1	–	–	–	–	–	–	–	−70.4	−83.0	−83.0	−70.5	−76.5	5.2
	+100.0	+81.7	+107.0	–	–	+92.6	–	–	–	–	–	–	–	+95.3	+87.1	+96.7	+103.1	+95.4	8.3
∗49933.581	−2.3	−10.9	+5.6	–	–	−0.1	–	–	–	–	–	–	–	−1.4	−4.6	0.0	+2.8	−1.4	4.9
49934.577	–	+66.2	+81.6	–	–	+78.0	–	–	–	–	–	–	–	+74.4	+64.8	+78.1	+83.6	+75.2	7.3
	–	−84.3	−76.9	–	–	−80.3	–	–	–	–	–	–	–	−84.3	−88.2	−86.6	−79.2	−82.8	4.1
49935.605	−75.4	−79.5	–	–	–	−73.3	–	–	−76.3	–	–	–	–	−80.5	−80.9	−80.8	−74.5	−77.6	3.1
	+86.4	+101.5	–	–	–	+90.3	–	–	+80.5	–	–	–	–	+89.5	+77.8	+91.0	+91.4	+88.5	7.3
∗49936.657	+3.4	–	−2.3	+6.7	–	−6.1	–	–	−0.1	–	–	−11.7	+7.6	–	−4.9	+3.3	+4.6	0.0	6.2
49937.587	–	–	+76.0	–	–	+69.4	–	–	–	–	–	+71.2	–	+76.4	+64.7	+67.6	+78.4	+71.9	5.1
	–	–	−76.5	–	–	−72.0	–	–	–	–	–	−75.9	–	−74.8	−72.8	−70.1	−70.6	−73.2	2.5
50239.906	–	–	–	–	–	−74.9	–	–	–	–	–	–	–	–	−72.1	−77.1	−72.1	−74.0	2.4
	–	–	–	–	–	+72.7	–	–	–	–	–	–	–	–	+84.1	+75.7	+74.9	+76.8	5.0
∗50240.883	–	−0.5	+12.6	–	–	+2.5	–	–	–	–	–	+3.1	+3.0	−0.4	−3.7	+2.5	+1.0	+2.2	4.5
50241.823	–	–	–	–	–	+88.0	–	–	–	–	–	+76.3	–	+81.8	+75.5	+86.8	+86.9	+82.5	5.6
	–	–	–	–	–	−79.7	–	–	–	–	–	−81.5	–	−98.3	−94.5	−101.0	−90.7	−90.9	8.7
∗50243.894	−0.5	+3.1	+8.0	–	–	+0.9	–	–	+2.8	–	–	+1.6	–	−4.0	−4.1	−5.7	+3.6	+0.5	4.2
50244.902	–	–	–	–	–	+74.2	–	–	–	+83.1	–	+75.9	–	+79.1	+65.6	+58.3	+72.5	+72.6	8.6
	–	–	–	–	–	−69.9	–	–	–	−79.1	–	−79.5	–	−75.8	−72.9	−80.5	−78.0	−76.5	3.9
50245.857	−87.9	−59.5	–	–	–	−74.3	–	–	–	–	–	−75.7	–	−76.2	−69.7	–	−80.0	−74.7	8.8
	+78.6	+93.9	–	–	–	+75.2	–	–	–	–	–	+79.7	–	+84.6	+80.7	–	+84.8	+82.5	6.0
50293.763	−86.2	–	−72.6	–	–	−69.5	–	–	–	−64.7	–	−72.1	–	−78.0	−76.9	−81.4	−69.0	−74.5	6.7
	+70.8	–	+89.5	–	–	+87.4	–	–	–	+92.5	–	+86.3	–	+80.7	+72.5	+73.4	+89.8	+82.5	8.4
∗50295.770	+6.4	+12.5	–	–	–	+4.1	–	–	–	–	–	+8.4	–	–	–	–	+4.2	+7.1	3.5
50296.787	–	–	–	–	–	–	–	–	–	–	–	–	–	−66.4	−66.2	−66.1	−54.3	−63.2	5.9
	–	–	–	–	–	–	–	–	–	–	–	–	–	+62.3	+63.5	+66.5	+65.1	+64.3	1.8
∗50298.730	–	–	–	–	–	+0.4	–	–	–	+16.7	–	+7.9	–	–	–	–	+18.9	+11.0	8.5
∗50348.614	−8.4	−3.3	−0.9	–	−5.9	+0.4	–	–	–	–	−12.2	−1.6	–	−6.9	−0.5	−14.0	−2.5	−5.1	4.8
50671.471	−73.1	−78.9	−70.9	–	–	−75.0	–	–	−75.4	–	–	−81.0	–	–	−83.1	−87.6	–	−78.1	5.6
	+92.5	+82.6	+94.0	–	–	+102.6	–	–	+96.0	–	–	+98.2	–	–	+87.4	+99.1	–	+94.0	6.5
∗50672.494	–	–	–	–	–	–	–	–	–	–	–	−14.5	−0.5	−2.1	+0.2	−12.1	−0.5	−4.9	6.6
∗51713.844	−1.0	−23.4	−5.0	–	–	−3.3	–	–	–	–	–	−12.8	–	−1.9	+4.4	−5.4	+0.7	−5.3	8.3
51714.835	–	−86.6	−86.9	–	–	−83.0	–	–	–	–	–	−82.7	–	–	−91.2	−92.6	−87.5	−87.2	3.7
	–	+110.1	+102.3	–	–	+104.8	–	–	–	–	–	+105.0	–	–	+94.9	+99.9	+103.4	+102.9	4.7

Table 2 (continued)

HJD 2 400 000+	He I 3819	He I 4026	Si IV 4088	He II 4200	He I 4387	He I 4471	Mg II 4481	He II 4542	He II 4686	He I 4713	He I 4921	He I 5015	He II 5411	O III 5592	C IV 5801	C IV 5812	He I 5875	V_R km s^{-1}	σ km s^{-1}
51714.862	–	–	–	–	–	–	–	–	–	–	–	–	−91.5	−106.0	−88.7	−95.2	−86.0	−93.5	7.8
	–	–	–	–	–	–	–	–	–	–	–	–	+80.3	+110.0	+98.5	+104.0	+103.4	+99.2	11.3
∗51715.548	−1.2	−4.4	+6.4	–	–	+3.8	–	–	–	–	+6.5	+5.4	+0.8	−0.1	−4.2	−4.7	3.5	+1.1	4.3
∗51715.737	–	–	–	–	–	–	–	–	–	–	–	–	+1.0	+0.8	−1.6	+6.7	+1.0	+1.6	3.1
51715.796	–	–	–	–	–	–	–	–	–	–	–	+64.6	–	+66.9	+54.2	+55.1	+65.2	+61.2	6.0
	–	–	–	–	–	–	–	–	–	–	–	−58.0	–	−64.5	−62.7	−67.2	−61.9	−62.9	3.4
51716.570	+72.0	–	+74.8	–	–	+79.0	–	–	–	–	+75.4	+73.0	–	+69.6	+65.6	+66.0	+69.4	+71.6	4.4
	−75.6	–	−67.4	–	–	−70.0	–	–	–	–	−61.7	−71.7	–	−69.3	−66.7	−68.1	−66.4	−68.5	3.8
51716.656	–	–	–	–	–	–	–	–	–	–	–	–	–	+38.8	+39.5	–	+23.7	+34.0	8.9
	–	–	–	–	–	–	–	–	–	–	–	–	–	−35.1	−40.5	–	−50.2	−41.9	7.6
∗51716.778	−18.1	−15.2	−4.2	–	–	−10.1	–	–	–	−13.1	–	−12.4	–	–	−14.0	−1.6	−11.8	−11.2	5.2
51717.609	−68.4	−83.0	−79.0	–	–	−77.2	–	–	−85.5	–	–	−85.4	–	−83.2	–	–	−82.7	−80.5	5.7
	+94.2	+101.7	+103.6	–	–	+95.8	–	–	+93.7	–	–	+92.2	–	+91.6	+91.4	–	+96.4	+95.6	4.4
51717.727	–	–	–	–	–	–	–	–	–	–	–	–	−85.4	−95.9	−91.0	–	−89.5	−90.5	4.3
	–	–	–	–	–	–	–	–	–	–	–	–	+83.0	+97.2	+100.9	–	+100.1	+95.3	8.3
51717.829	−99.6	−99.3	–	–	–	−85.8	–	–	–	−97.7	–	−84.8	–	−89.2	−90.6	−96.7	−93.6	−93.0	5.7
	+90.4	+90.0	–	–	–	+102.0	–	–	–	+100.8	–	+98.8	–	+98.0	+97.1	+101.0	+101.4	+97.7	4.6
52066.791	–	−71.1	−64.2	−67.8	–	−59.0	–	–	–	–	−75.5	−87.5	−64.9	−65.2	–	–	−75.4	−70.1	8.5
	–	+83.9	+106.0	–	–	+94.0	–	–	–	–	+83.5	+107.5	+87.0	+83.0	–	–	+79.9	+90.6	10.8
52067.768	–	+81.3	–	–	–	+103.0	–	–	–	–	–	–	–	–	–	–	+102.5	+95.6	12.4
	–	−109.5	–	–	–	−109.0	–	–	–	–	–	–	–	–	–	–	−113.0	−110.5	2.2
52069.730	−69.0	−73.5	−78.4	−70.6	–	–	−75.2	–	–	–	−69.4	−81.1	–	−85.1	–	–	−76.0	−75.4	5.8
	+76.1	+65.6	+96.7	+114.3	–	+87.4	+87.8	–	–	–	+76.2	+88.3	–	–	–	–	+86.9	+86.6	13.8
52069.794	−67.0	−79.2	−70.0	–	−62.4	−61.7	–	–	–	–	–	–	−56.4	−69.1	–	–	−72.6	−67.3	7.1
	+74.4	+58.3	+89.4	–	+107.1	+68.6	–	–	–	–	–	–	+72.4	+67.0	–	–	+72.1	+76.1	15.2
52070.621	–	+101.1	+90.7	–	+102.4	+96.6	+78.9	+91.7	+87.0	–	–	+92.9	+98.9	+93.9	+92.9	+92.7	+93.8	+93.3	6.1
	–	−90.4	−98.6	–	−106.2	−95.3	−99.8	−81.4	−92.9	–	–	−110.4	−93.5	−99.7	−97.4	–	−98.7	−97.1	7.4
52070.731	+101.6	+100.8	+110.2	–	–	+111.1	+88.7	–	+95.7	+107.2	–	–	+106.3	+104.4	+109.1	–	+103.7	+103.5	6.7
	–	−118.2	−107.7	–	–	−104.3	−106.1	−90.9	−103.4	−94.6	–	–	−91.0	−111.8	−114.3	–	−111.7	−104.9	9.3
52070.792	–	+92.4	+107.0	–	–	+110.2	+100.5	+95.2	+97.4	+117.8	+92.6	+105.0	+103.3	+104.7	–	–	+107.6	+102.8	7.6
	–	−111.0	−112.3	–	–	−104.5	−115.0	−99.0	−106.8	−96.0	−110.4	−113.9	−92.3	−115.8	–	–	−111.4	−107.3	7.8
∗52071.663	+2.3	−2.3	+2.7	+4.5	+6.0	+6.8	−1.3	+6.6	+4.4	+14.0	+5.4	+7.4	+2.8	−3.3	+0.2	−0.3	+4.9	+3.5	4.2
∗52071.746	+3.9	+0.7	+15.0	+13.6	+13.4	+7.9	+2.1	+5.0	+4.7	+12.5	+10.6	+1.0	+2.0	+0.3	+2.6	+12.4	+3.7	+6.5	5.2
∗52071.810	+7.4	−2.8	+16.0	+5.5	−1.2	+2.7	+5.5	+0.9	+6.7	+5.5	+22.2	+19.2	+2.6	−9.0	−0.2	+7.6	+5.5	+5.5	7.8
52072.663	–	−71.3	−87.3	–	−95.0	−67.5	–	–	−80.5	−63.4	–	−79.2	−76.9	−62.7	−75.3	−70.0	−74.8	−75.3	9.4
	–	+88.9	+98.4	–	+93.0	+88.8	–	–	+77.6	–	+101.2	+99.6	+90.6	+80.0	+90.2	+87.0	+86.1	+90.1	7.2
52072.717	−67.9	−71.1	–	–	–	−75.1	−61.2	–	–	–	–	–	−65.3	−68.7	−71.2	–	−75.0	−69.4	4.7
	–	+80.2	–	–	–	+73.0	–	–	–	–	–	–	+79.4	+77.7	+79.6	+86.2	+76.1	+78.9	4.1

∗ Value omitted from orbital solution

Table 3. Radial velocity measurements considered in the orbital solution of HD 165052.

HJD 2 400 000+	Phase ϕ	V_1 km s^{-1}	O-C km s^{-1}	n_1	V_2 km s^{-1}	O-C km s^{-1}	n_2
49854.640	0.210	+88.2	−4.1	4	−98.5	+1.3	4
49931.634	0.265	+69.2	−5.9	8	−91.4	−10.6	8
49932.663	0.613	−76.5	+1.7	8	+95.4	+6.7	8
49934.577	0.261	+75.2	−1.5	7	−82.8	−0.3	7
49935.605	0.609	−77.6	−0.4	8	+88.5	+1.0	8
49937.587	0.280	+71.9	+2.6	7	−73.2	+1.2	7
50239.906	0.583	−74.0	−4.1	4	+76.8	−2.7	4
50241.823	0.232	+82.5	−3.9	6	−90.9	+2.4	6
50244.902	0.274	+72.6	+1.5	7	−76.5	+0.2	7
50245.857	0.597	−74.7	−0.6	7	+82.5	−1.6	7
50293.763	0.809	−74.5	−4.6	9	+82.6	+3.1	9
50296.787	0.832	−63.2	−3.2	4	+64.3	−4.2	4
50671.471	0.624	−78.1	+2.8	8	+94.0	+2.4	8
51714.835	0.697	−87.2	+2.7	7	+102.9	+1.3	7
51714.862	0.706	−93.5	−3.6	5	+99.2	−2.4	5
51715.796	0.022	+61.2	+0.4	5	−62.9	+2.1	5
51716.570	0.284	+71.6	+4.1	9	−68.5	+3.9	9
†51716.656	0.313	+34.0	−	3	−41.9	−	3
51717.609	0.635	−80.7	+2.5	9	+95.6	+1.4	9
51717.727	0.675	−90.5	−1.7	4	+95.3	−5.0	4
51717.829	0.710	−93.0	−3.2	9	+97.7	−3.8	9
52066.791	0.798	−70.1	+3.7	9	+90.6	+6.7	8
52067.768	0.129	+95.6	−2.9	3	−110.5	−3.8	3
52069.730	0.792	−75.4	+0.3	9	+86.6	+0.7	9
52069.794	0.814	−67.3	+0.5	7	+76.2	−1.0	7
52070.621	0.094	+93.3	+1.3	12	−97.1	+2.4	13
52070.731	0.131	+103.5	+4.7	11	−104.9	+2.0	11
52070.792	0.152	+102.8	+3.1	12	−107.4	+0.5	12
52072.663	0.785	−75.3	+2.7	12	+90.1	+1.7	12
52072.717	0.803	−69.4	+2.6	7	+78.9	−2.9	7

† Value discarded from the final solution due to pair blending

3.2 The radial-velocity orbit

To determine an improved orbital period for the HD 165052 binary system we used all the available radial velocities of this star, i.e., those derived from our new high-resolution CCD observations, those obtained by Morrison & Conti (1978) from photographic spectra, which were reassigned in accordance with the new period, and those derived by Stickland et al. (1997) from *IUE* observations. The applied period-finding routines, which comprised the Lafler & Kinman (1965) method and several subsequent modifications of it (e.g. Marraco & Muzzio 1980 and Cincotta, Méndez & Núñez 1995), led to a most probable value of $P = 2.95510 \pm 0.00002$ days, very close to the value determined by Stickland et al. (1997), namely 2.95506 ± 0.00001.

The orbital elements were obtained from the new high-resolution radial velocities only, using a modified version of the code originally written by Bertiau & Grobben (1969), considering simultaneously the radial-velocity measurements for both binary components. One of the 30 double-lined spectra was discarded from the final solution because of the pair blending effect.

The resulting orbital elements are listed in Table 4. We have found a slight eccentricity, $e = 0.09$, which is almost certainly real since trial solutions with the eccentricity fixed to 0.0 yield systematic shifts between the fitted curve and the observations, and the probable error derived is $\sim 5\,\mathrm{km\,s^{-1}}$, more than double the error of the adopted eccentric orbit fit. Moreover, in accordance with the criterion developed by Lucy & Sweeney (1971) for deciding between an elliptical and a circular orbit, the eccentricity will be signficant at the 5 % level if it exceeds 3.63 times its probable error, which is widely satisfied in this case.

Figure 1 shows the observed radial velocities along with the orbital solutions of Table 4.

Figure 2 (left-hand panel) shows the radial-velocity curves determined from our high-resolution data in comparison with previous observations (Morrison & Conti 1978 and Stickland et al. 1997). The significant shift between the orbital solution obtained from the new data set and the previous observations might be an indication of apsidal motion. Apsidal motion changes the shape of the radial-velocity of a binary curve when observed at different epochs, as described, for example, by Morrell et al. (2001) for the orbit

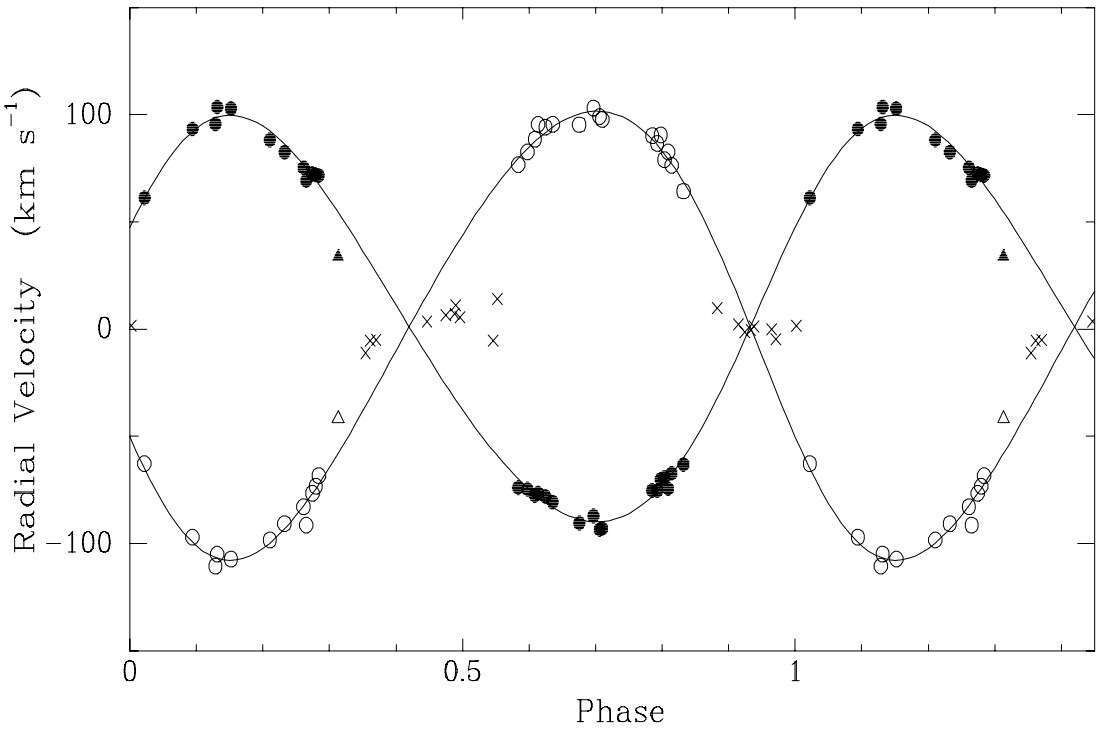

Figure 1. The spectroscopic orbit of HD 165052 determined from high resolution CASLEO observations. Filled and open symbols represent the primary and secondary components, respectively. Triangles denote measurements not considered in the solution because of pair blending and crosses depicts data where no double lines are observed.

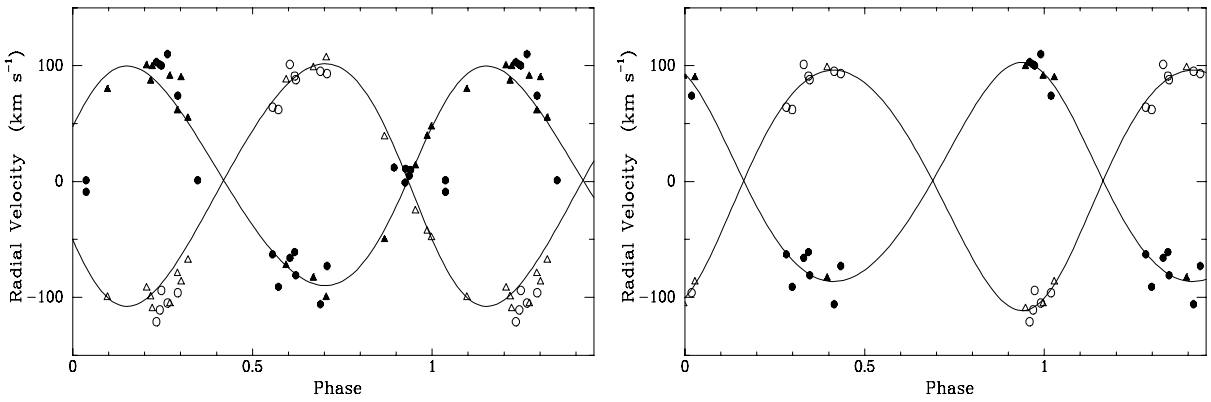

Figure 2. Left-hand panel: previously published data in comparison with the spectroscopic orbit computed from our observations. Filled and open triangles represent radial velocities derived from *IUE* data (Stickland et al. 1997) for the primary and secondary components, respectively. Circles represent the optical velocities from Morrison & Conti (1978). Right-hand panel: orbital solution computed from the observations previous to 1982, adopting the period and eccentricity obtained in this work. Filled symbols represent the primary component and open symbols the secondary one, with circles denoting optical and squares IUE velocities.

of HD 93205. The precise knowledge of apsidal rotation in a binary system is important as it may provide a way to find an independent estimate of the masses of the binary components (see Benvenuto et al. 2002). Consequently, we decided to investigate this hypothesis, calculating an orbital solution for a data subset containing the oldest observations, i.e., previous to 1982, adopting the values of $P = 2.95510$ days and $e = 0.09$ computed in this work for the orbital period and the eccentricity.

As a result, we found that the old observations fit the new orbit derived from high-resolution echelle spectra, if one only varies the longitude of periastron ω. The value ω that best describes the binary motion between 1973 and 1982 is $\omega = 26\overset{\circ}{.}4 \pm 19\overset{\circ}{.}6$ instead of $\omega = 296\overset{\circ}{.}7 \pm 3\overset{\circ}{.}5$ resulting from the new calculation. This solution is illustrated in Figure 2 (right-hand panel). The probable error of this fit is only $6.3\,\mathrm{km\,s^{-1}}$.

With the above-determined orbital solution and taking the estimates for $V_e \sin i$ found from *IUE* spectra by Stickland et al. (1997), i.e., 85 and 80 $\mathrm{km\,s^{-1}}$ for the primary

Table 4. Orbital elements of HD 165052 binary components derived from radial velocities measured in high-resolution spectrograms

P (days)	2.95510 ± 0.00001
e	0.09 ± 0.004
ω (°)	296.7 ± 3.5
T_o (HJD)	2449871.75 ± 0.03
$T\,V_{max}$ (HJD)	2449872.19 ± 0.03
V_o (km s^{-1})	1.05 ± 0.31
K_1 (km s^{-1})	94.8 ± 0.5
K_2 (km s^{-1})	104.7 ± 0.5
$a_1 \sin i$ ($R_\odot$)	5.51 ± 0.03
$a_2 \sin i$ ($R_\odot$)	6.09 ± 0.03
$M_1 \sin^3 i$ ($M_\odot$)	1.26 ± 0.03
$M_2 \sin^3 i$ ($M_\odot$)	1.14 ± 0.03
Q (M_2/M_1)	0.90 ± 0.01
Prob. error (km s^{-1})	2.21

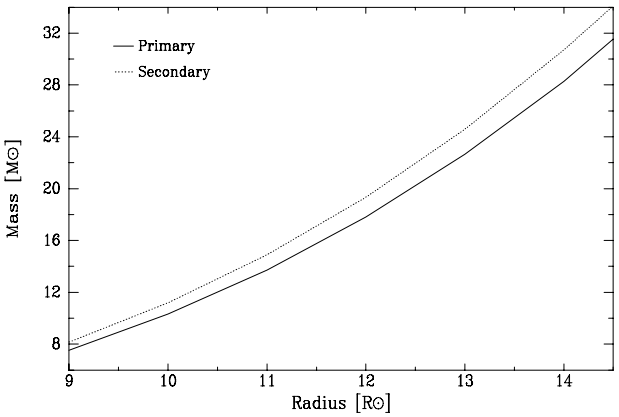

Figure 3. Mass-radius relationship for HD 165052 assuming synchronously rotating stars.

and secondary components respectively, we derived a mass-radius relationship for a system of two synchronously rotating stars. The resulting curves, $M_1 = 0.010309 \times R_1^3$ and $M_2 = 0.011189 \times R_2^3$, are shown in Figure 3. As the binary components are both dwarfs (see next section for details), one expects individual radii of $\sim 10\ R_\odot$ (Vacca et al. 1996), which would indicate masses close to $10 M_\odot$ for each component. These values are obviously too low for O-type stars, and the reason for this inconsistency is probably the hypothesis of synchronization. Mass estimates for early O-type stars are still controversial. If the masses are in the expected range for the corresponding spectral types (30-40 $M_\odot$), the orbital inclination would be around $i = 20°$, leading to rotational velocities near 250 km s^{-1}. This would imply rotation periods of about 2 d in both cases. It is worthwhile to mention that the *Hipparcos* photometry shows no evidence of variability in excess of 0.01 magnitude with the orbital period,

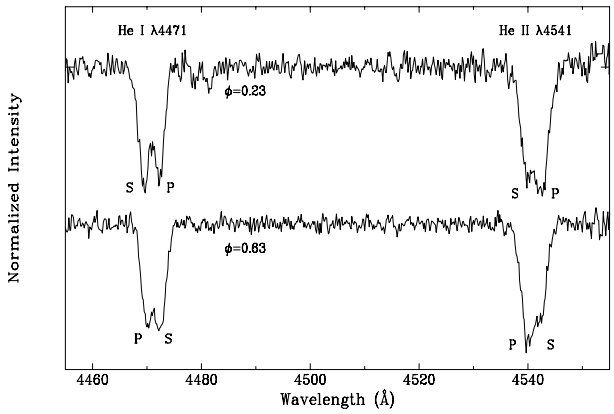

Figure 4. Rectified spectrograms of HD 165052 in the region of the He I 4471 Å and He II 4542 Å absorption lines at nearly opposite orbital phases. "P" and "S" refer to the primary and secondary components, respectively.

in good agreement with the expectations for the system's small inclination and under-Roche filling stellar radii.

4 SPECTRAL CLASSIFICATION AND EMISSION LINES

HD 165052 has often been considered as a system composed of two stars identical in spectral type, i.e. O6.5 V + O6.5 V or more recently O6 V + O6 V (Penny 1996), but what emerged from the analysis of our high-resolution CCD spectra is that one of the components (the primary in mass terms) is earlier than the other, although the difference corresponds to no more than one spectral subclass. Thus, the primary component shows a spectrum in which the ratio He II λ4542/He I λ4471 is larger than unity and corresponds to the spectral type O6.5 V. On the other hand, in the secondary spectrum the He I absorption lines are slightly stronger than the He II lines, and the ratio He II λ4542/He I λ4471 is somewhat lower than unity, indicating a spectral type O7.5 V. Figure 4 displays the region containing the He I 4471 Å and He II 4542 Å absorption lines in two high-resolution échelle spectrograms at opposite phases of the binary period. Also apparent in Figure 4 is a phase-dependent change in the intensity of the absorption lines of the secondary component which will be discussed in the next section.

According to the O-type optical luminosity criteria (Walborn & Fitzpatrick 1990), at spectral classes O6 to O8, one finds He II λ4686 Å in strong absorption on the main sequence; in the intermediate luminosity classes this absorption line weakens and may become neutralized; and finally, the O supergiants have this feature strongly in emission. A correlative increase with luminosity in the strengths of the Si IV absorption lines flanking Hδ can also be seen at these spectral types. We find both phenomena in the spectrum of HD 165052 (see Figure 6 later), indicating that it must be a class V system.

We also searched the *IUE* database and retrieved all the available observations of HD 165052, along with those corresponding to HD 190864 and HD 93146 presented as O6.5 III(f) and O6.5 V((f)) prototypes respectively, in the

atlas of ultraviolet spectra by Walborn, Nichols-Bohlin & Panek (1985).

A simple inspection of those ultraviolet spectra showed that the stellar-wind profile of the Si IV doublet at 1394 − 1403 Å, which displays a pronounced luminosity dependence with no effect at class V and adquiring a P Cygni type profile at higher luminosities, is completely absent in the spectrum of HD 165052. The same occurs with the profile of N IV 1720 Å, which shows a full P Cyg profile at III(f) but no trace of winds in the dwarf spectra. Moreover, the stellar-wind profiles of the doublets N V 1239−1243 Å and C IV 1548−1551Å are much less developed in the spectrum of HD 165052 than in the spectrum of the giant HD 190864 (see Figure 5). These considerations add more evidence in support of the classification of HD 165052 as a class V system.

An interesting point concerns the reddening in the region. McCall, Richter & Visvanathan (1990) found the anomalous value of $R = 4.6 \pm 0.3$ for the reddening law in the Lagoon Nebula, and it is apparently uniform throughout the region. However, this value of R leads to an absolute visual magnitude $M_V = -5.71$ for each binary component (see Stickland et al. 1997), which would be appropiate for luminosity class III objects (Vacca et al. 1996; Schmidt-Kaler 1982). On the other hand, adopting a normal value of $R = 3.2$, together with the color excess $E(B-V) = 0.43$ estimated for HD 165052 and a distance modulus of $11\overset{\mathrm{m}}{.}25$ (Sung et al. 2000), one finds for the binary system $M_V = -5.76$. Assuming that both components contribute with equal flux, this implies $M_V = -5.0$ for each one, in fair accord with the values assigned to O6.5 V stars in the above mentioned calibrations.

Many of the massive stars also show certain emission lines related to luminosity. This characteristic is usually identified by adding the designation "f" to the spectral type. Main-sequence spectra in the range O6-O7 present strong He II λ4686 Å absorption and often weak N III $\lambda\lambda$4634-40-42 emission, which corresponds to the notation ((f)) according to Walborn's (1971) classification criteria. In addition, one frequently finds a very weak C III λ5696 emission in types from O4 to O8 (Walborn 1980). These emissions being quite weak, their detection is strongly affected by observational parameters. The new CCD observations of HD 165052, with $S/N \sim 300$ but $\lambda/\Delta(\lambda)$ only 1800, do not show the N III $\lambda\lambda$ 4634-40-42 emission reported by Walborn (1973) (see Figure 6). However, after careful inspection of the corresponding photographic observation obtained at Cerro Tololo Inter-American Observatory in 1972, which was kindly provided by Dr. Walborn, we are able to confirm the existence of those emission lines, although very weak, in the spectrum of HD 165052. On the other hand, the presence of C III λ5696 emission is shown in Figure 6. From the analysis of the complete set of échelle spectra, we discovered that this feature is actually a double line which shares the binary motion of both components of HD 165052, thus demonstrating that the C III emission arises in both stars and not only in the primary as was suggested by Conti (1974) (Figure 7). Also, the primary component of this emission line is stronger than the secondary. Also evident from Figure 6 is the strength of the He II 4686 Å absorption, indicating an early evolutionary state (main sequence or zero age main sequence) for this system.

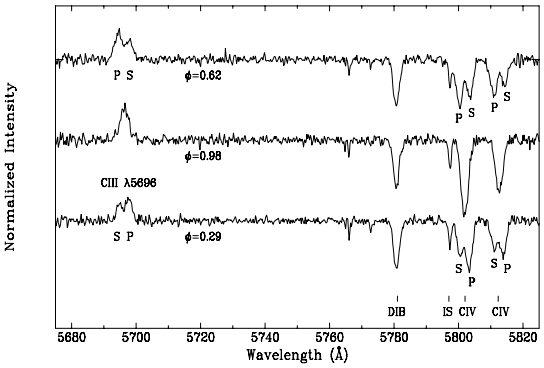

Figure 7. Rectified spectrograms of HD 165052 at three different orbital phases showing the duplicity of the C III λ5696 emission line. The C IV absorption lines λ5801 and λ5812 are also displayed in this figure.

5 WIND-WIND INTERACTION

Massive luminous stars are known to be sources of strong stellar winds. In early close binary systems the individual stellar winds may collide in a bow shock zone between the stars. This idea is strongly supported by the growing observational evidence from investigations of Hα (Thaller 1997), UV wind lines (Koch et al. 1996) and X-ray emission properties (Corcoran 1996; Pittard & Stevens 1997) in binaries containing O-type stars.

Since HD 165052 is a short-period binary with luminous components, it is a good candidate to show wind-wind collision effects.

One observational consequence of the presence of wind interactions in a massive binary is the detection of Hα emission. Formed in the shock region, this emission may display velocity variations defined by the structure of the circumstellar gas, and thus one expects to observe phase-dependent variations in the line profile.

Thaller (1997) conducted a search for Hα emission in a large number of binaries with O-type components, including HD 165052, for which she found no sign of emission or visible distortion in the Hα line profile.

We obtained five high-resolution spectra centered at Hα in different orbital phases. We measured the equivalent widths of the Hα line profile finding no significant variations. Consequently, we are unable to confirm the existence of phase-related changes in this line. To draw a conclusion, it will be necessary to expand the available data set with spectra corresponding to several distinct orbits, in order to be able to appreciate possible orbit-to-orbit profile variations. Also, as was pointed out by Thaller (1997), there is little expectation to detect Hα line-profile variations, as there seems to be a strong correlation between the emission and the evolutionary phase of the primary star, this phenomenon being very rare in systems with main-sequence components.

From the minimum masses quoted in Table 4, we can infer that the orbital inclination is low, and thus the colliding wind effect may not be conspicuous.

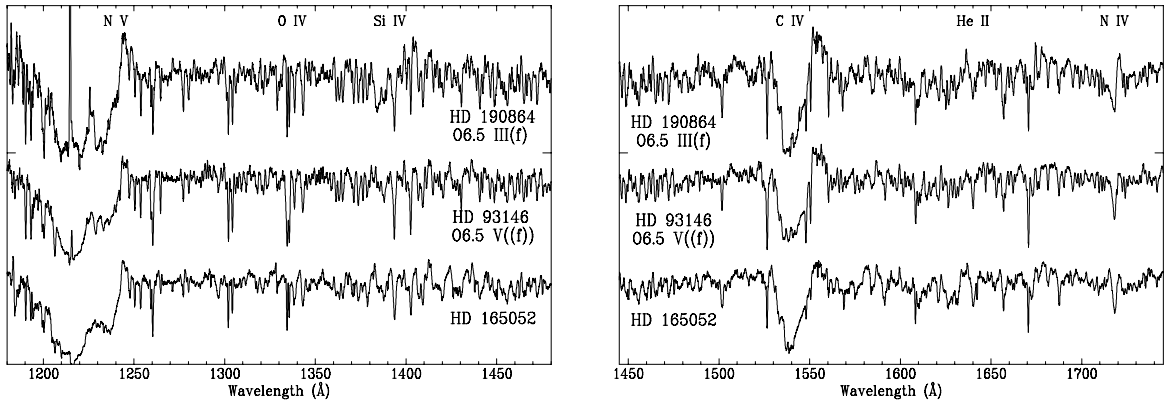

Figure 5. *IUE* spectra of HD 165052 and the classification standards HD 190864 and HD 93146. A thorough comparison among them brings more evidence in support of the luminosity class V for the binary components.

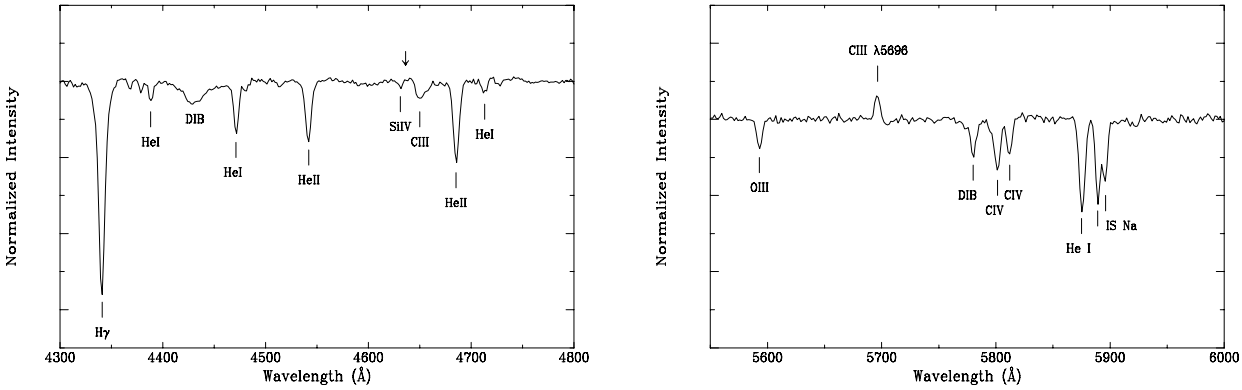

Figure 6. Low-dispersion spectra of HD 165052. N III λλ4634-40-42 emissions should be observed where the arrow indicates (left-hand panel). C III λ5696 emission is clearly observed above the continuum (right-hand panel).

5.1 The X-ray lightcurve of HD 165052

In a massive binary, X-ray emission is observed as a natural consequence of wind-wind interaction that produces a hot shocked gas region with temperatures in excess of a million degrees. The density and relative velocity of the winds in the collision region and the wind absorption along the line of sight all vary as the stars revolve in their orbits. Depending directly on those parameters, one expects a phase-dependent change in the observed X-ray emission (Corcoran 1996 and references therein).

An X-ray light curve of HD165052 based on pointed observations with the ROSAT Position Sensitive Proportional Counter (PSPC) was obtained by Corcoran (1996), and although this lightcurve was constructed using the ephemerides from Morrison & Conti (1978), it shows a significant variability apparently tied to orbital phase.

Using our new determination of the period, we phased the ROSAT PSPC observations in order to re-examine the X-ray light curve of HD 165052.

As seen in Figure 8, the light curve thus obtained shows clear phase-locked variations consisting of a rise of the observed X-ray flux near both quadratures, i.e., $\phi = 0.22$ and $\phi = 0.72$ approximately.

This twin-peaked structure of the X-ray emission is entirely consistent with the theoretical model developed by Pittard & Stevens (1997) of colliding winds in an O+O binary system, in which the winds of each star have similar momentum. They explained the variation in the observed X-ray flux mainly as the result of changing absorption along the line of sight suffered by the intrinsic X-ray luminosity at different phases of the binary motion. The occultation of

Table 5. ROSAT PSPC observations of HD 165052. The values listed in the third column represent a simple average of all the observations obtained during the same Julian day. The fourth column shows the corresponding errors. The orbital phases were computed with the ephemeris presented in Table 4.

HJD 2440000+	Phase ϕ	Rate (PSPC counts s^{-1})	σ
8332.6553	0.174	0.063	0.011
8900.1735	0.221	0.067	0.021
8901.7591	0.757	0.064	0.014
8904.0855	0.545	0.055	0.017
9878.5524	0.302	0.037	0.011
9079.4175	0.877	0.037	0.013
9079.5420	0.919	0.026	0.010

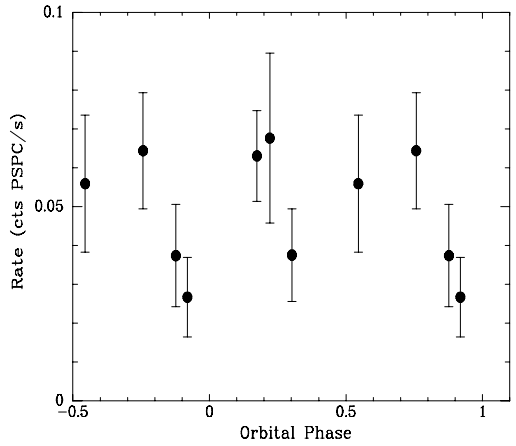

Figure 8. X-ray ligth curve of HD 165052.

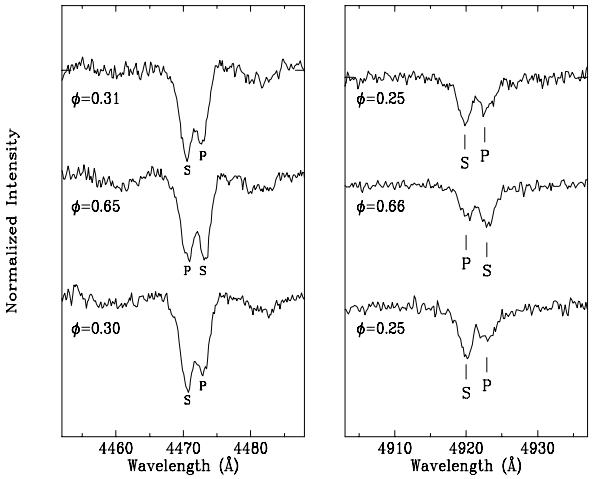

Figure 9. Rectified spectrograms of HD 165052 at three orbital phases illustrating the Struve-Sahade effect observed in the He I 4471Å (left-hand panel) and 4921 Å (right-hand panel) absorption lines. "P" and "S" tick marks show the primary and secondary components respectively.

the shocked region by the stars has a minor contribution. We therefore conclude that the effect of colliding winds is significant in this system, although attenuated by the unfavorable orbital inclination.

5.2 The Struve-Sahade Effect

The Struve-Sahade (S-S) effect is observed in many massive double-lined binaries and consists in the apparent strengthening of the lines of the secondary during orbital phases in which this component is approaching. Reported for the first time by Bailey (1896) in the lines of μ_1 Sco, this phenomenon was noted and studied in a number of hot binaries by Sahade (1962), Bagnuolo et al. (1997), Howarth et al. (1997) among other investigators.

The origin of the Struve-Sahade effect still remains unclear, since there are a variety of mechanisms that can result in the variations of the line intensities of both binary components as function of the orbital phase. In O+O binary systems expected to contain colliding stellar winds, in accordance with the model proposed by Gies, Bagnuolo & Penny (1997), the S-S effect may be explained by a mechanism of localized photospheric heating induced by the wind-collision. If the wind momentum of the primary dominates, the colliding-wind bow shock may reach close to the photosphere of the secondary and the X-ray flux arising from the shock region will preferentially heat one of the hemispheres of this star. Because of the Coriolis deflection due to orbital motion, the heated surface is best seen when the secondary is moving toward the observer. Thus, the contribution of the secondary to the binary spectrum is increased, yielding deeper secondary lines during the approaching phases.

As pointed out above, with a short period and very luminous components, HD 165052 appears as a potential candidate for colliding stellar winds, an idea strongly reinforced by the properties of the observed X-ray emission. Furthermore, from the ratio of the equivalent widths of well separated lines in the binary components, we estimated the visual luminosity ratio of the system through Petrie's method (Petrie 1940). Using for comparison the equivalent widths from Mathys (1988) corresponding to single stars of the same spectral types, we obtained from the He II 4542 Å and He II 4686 Å lines, $L(\mathrm{O6.5\,V})/L(\mathrm{O7.5\,V}) \sim 0.79 \pm 0.05$, indicating that the secondary has weaker wind than the primary. In view of this, the possibility of detecting the S-S effect in the binary spectrum arises naturally (in spite of the relatively low orbital inclination). We therefore examined our high-resolution spectra in detail, carefully comparing one quadrature with the other in order to detect systematic differences in the relative strength of the lines observed in the approaching and the receding phases.

We found variable line strength in several He I absorption lines. Figure 9 displays normalized spectrograms around the He I 4471 Å and 4922 Å absorption profiles at different orbital phases, where the effect can be appreciated. In fact, for example, in He I 4471 Å, the secondary-to-primary line depth ratio, which is near unity for orbital phase $\phi \sim 0.65$, appears to increase to a value significantly larger for phase $\phi \sim 0.30$. This absorption-line behavior provides an illustration of the S-S effect and consequently evidence supporting photospheric heating by the action of colliding winds in HD 165052.

6 SUMMARY AND CONCLUSIONS

In this paper we have presented a detailed study of the O-type binary system HD 165052 based on recent high-resolution CCD spectroscopic observations.

We have re-determined the spectral types of both binary components, resulting in the spectral classification of O6.5 V + O7.5 V. We have also detected the C III λ5696 emission in both spectral components, this line being stronger in the primary.

We have determined an improved set of orbital elements using our high-resolution optical spectra. We thus found a slightly eccentric orbit ($e = 0.09$) with a period of 2.95510 d, which is consistent with the previous determination from archival *IUE* observations performed by Stickland et al. (1997). We obtained for the binary components veloc-

ity semi-amplitudes of 94.8 ± 0.5 km s^{-1} and 104.7 ± 0.5 km s^{-1}, resulting in a mass-ratio $Q = 0.9$. Significant evidence for apsidal motion in HD 165052 was also presented.

From the new orbital solution, together with the projected rotational velocities of the components derived by Stickland et al (1997) and the fact that both stars belong to luminosity class V, we showed that the system has not reached synchronous rotation.

Assuming M_V corresponding to the derived spectral types and luminosity class for the binary components of HD 165052, one finds that the reddening law in the region should be normal, in contrast with previous determinations.

Finally, we investigated the interaction of winds in HD 165052 through examination of a number of effects that provide evidence for colliding winds in close binary systems. We found no emission or visible distortion of the Hα profile, but we certainly confirmed the presence of phase-locked variations of the X-ray emission. The X-ray light curve obtained shows a twin-peaked structure with two maxima, one near each quadrature phase, in good agreement with current models for O+O systems with equal stellar winds (Pittard & Stevens 1997). We also detected the presence of the Struve-Sahade effect in the He I absorption lines, reinforcing the idea that colliding winds could be in fact significant in HD 165052.

ACKNOWLEDGEMENTS

We gratefully thank Nolan Walborn for kindly providing the photographic material analysed in this study, as well as for many useful suggestions and for improving the English in an earlier version of this paper.

We acknowledge use at CASLEO of the CCD and data acquisition system supported under US NSF grant AST-90-15827 to R.M. Rich, and want to thank the director and staff of CASLEO for the use of their facilities and kind hospitality during the observing runs.

RHB acknowledges financial support from Fundación Antorchas (Project No. 13783-5).

We want to thank our referee, Douglas Gies, for helpful suggestions.

REFERENCES

Bailey, S.I. 1896, Harvard Circ. 11
Bagnuolo, W.G., Gies, D.R., Riddle, R., & Penny, L.R. 1997, ApJ, 527, 353
Benvenuto, O.G., Serenelli, A.M., Althaus, L.G., Barbá, R.H., & Morrell, N.I. 2002, MNRAS, in press
Bertiau, F., & Grobben, J. 1969, Ric. Astron. Sp. Vaticana, 8, 1
Chlebowski, T., & Garmany, C.D. 1991, ApJ, 368, 241
Cincotta, P.M., Méndez, M., & Núñez, J.A. 1995, ApJ, 449, 231
Conti, P.S. 1974, ApJ, 187, 539
Corcoran, M.F. 1996, RMXAAC, 5, 54
Gies, D.R., Bagnuolo, W.G., & Penny, L.R. 1997, ApJ, 479, 408
Howarth, I.D., Siebert, K.W., Hussain, G.A.J., & Prinja, R.K. 1997, ApJ, 284, 265
Koch, R.H., Pachoulakis, I., Pfeiffer, R.J., & Stickland, D.J. 1996, RMXAAC, 5, 9
Lafler, J., & Kinman, T.D. 1965, ApJ S, 11, 216
Lucy, L.B., & Sweeney, M.A. 1971, AJ, 76, 544
McCall, M.L., Richer, M.G., & Visvanathan, N. 1990, ApJ, 357, 502
Marraco, H.G., & Muzzio, J.C. 1980, PASP, 92, 700
Mathys, G. 1988, A&A, 76,427
Morrell, N.I., Barbá, R.H., Niemela, V.S., Corti, M.A., Albacete Colombo, J.F., Rauw, G., Corcoran, M., Morel, T., Bertrand, J.-F., Moffat, A.F.J., & St-Louis, N. 2001, MNRAS, 326, 85
Morrison, N.D., & Conti, P.S. 1978, ApJ, 224, 558
Penny, L.R. 1996, Ph.D. thesis, Georgia State University
Petrie, R.M. 1940, Pub.DAO, 7, 205
Pittard, J.M., & Stevens, I.R. 1997, MNRAS, 292, 298
Plaskett, J.S. 1924, PDAO, 2, 287
Sahade, J. 1962, in Sahade J., ed., Symposium on Stellar Evolution. La Plata Obs., Buenos Aires, p. 185
Schmidt-Kaler, Th. 1982, "Landolt-Bornstein, NS", 2, 455
Stickland, D.J., Lloyd, C., & Koch, R.H. 1997, The Observatory 117, 295
Sung, H., Chun, M., & Bessell, M. 2000, AJ, 120, 333
Thaller, M.L. 1997, ApJ, 487, 380
Vacca, W.D., Garmany, C.D., & Shull, J.M. 1996, ApJ, 460, 914
Walborn, N.R. 1971, ApJ SS, 23, 257
Walborn, N.R. 1972, AJ, 77, 312
Walborn, N.R. 1973, AJ, 78, 1067
Walborn, N.R. 1980, ApJ SS, 44, 535
Walborn, N.R., & Fitzpatrick, E.L. 1990, PASP, 102, 379
Walborn, N.R., Nichols-Bohlin, J., & Panek, R.J. 1985, International Ultraviolet Explorer Atlas of O-type Spectra from 1200 to 1900 Å(Washington: NASA)
Walker, M.F. 1957, ApJ, 125, 636